Chapter 5

Tracking system with MEMS mirror

Up to now, this project has dealt with the theoretical optimization of the tracking servo with MEMS mirror through the use of simulation models. For these models used in the design of a practical system, it must accurately reflect the improved performance of the system when it is implemented in hardware. This chapter will look at the performance of the tracking servo hardware based on the analysis in Chapter 4. Ultimately, the tracking servo performance that matters most is how well the system keeps the laser spot tracked on a spinning optical disk that has a finite amount of focusing runout. Minimizing the tracking error and increasing rotation speed in this situation are, after all, the most important purpose of replacing voice coil motor with tracking mirror. The final test in this thesis then is to measure the tracking error for the optimized hardware prototype. The tracking performance is compared between systems with tracking mirror or with voice coil motor (VCM).

5.1 Implement of tracking system

The system diagram of the tracking-mirror control system is shown in Fig. 5-1. This system provides flexibility for running control experiments in tracking regardless of general voice coil motor or novel MEMS tracking mirror. The system comprised a tracking mirror, photo-detector, power driver, and PC based controller. Because PC can only receive and generate digital signals, the AD/DA card **[27]** is necessary to communicate between the practical system and the digital computer. The AD (analog-to-digital) converter is a device to sample the continuous signal voltage from the sensor and convert that signal to a digital word; the DA (digital-to-analog)

converter is a device to convert the digital word from the computer to an analog voltage. The computer is the device where the compensation is programmed and calculations are carried out. Therefore the tracking-mirror system use PC and NI AD/DA card to implement the PID controller simulated in previous chapter. The 200 kHz sampling rate and 12-bit quantizers of AD/DA card are high enough for computer to calculate and control accurately.

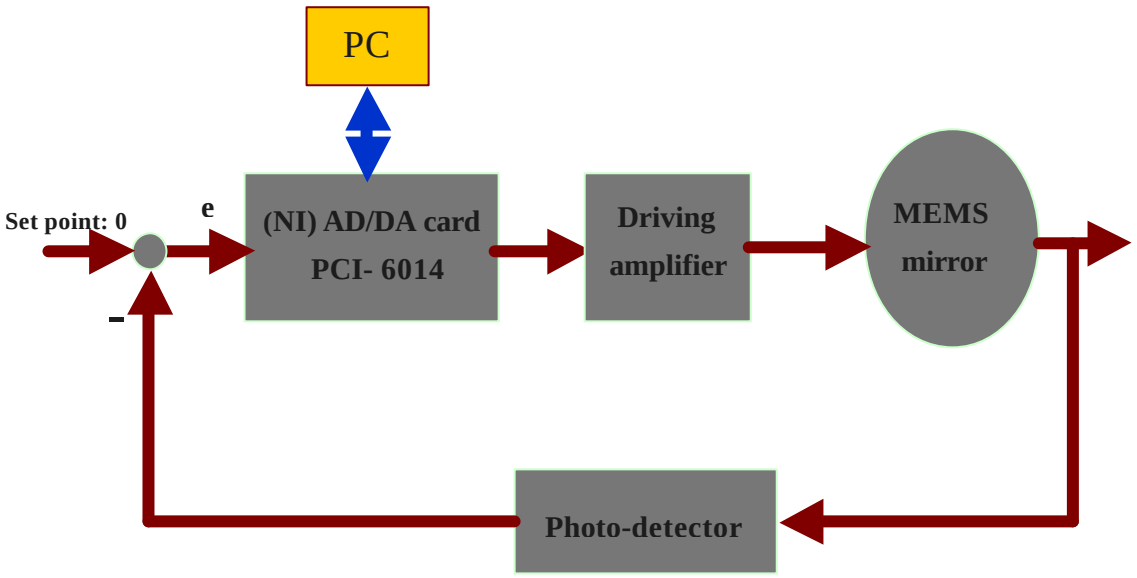

Fig. 5-1 The practical diagram of tracking system

5.1.1 Implement action of PID algorithm in LABVIEW software

In continuous systems the optimal controller has already been designed and simulated by using PID controller in Chapter 4. Therefore, the same ideas need be used in practice with AD/DA card and LABVIW software. This section describes how the LABVIEW codes implement the PID algorithm. The LABVIEW codes for implementing PID controller are as follows:

Error calculation

The following formula represents the current error used in calculating proportional, integral and derivative action.

$$e(k) = (SP - PV),$$

where SP is the setpoint and PV is the process variable.

Proportional

$$u(k) = K_c e(k) = K_P e(k),$$

Derivative

$$u(k) = K_c T_D \frac{de(k)}{dt} = K_D \frac{de(k)}{dt},$$

Integral

$$u(k) = \frac{K_c}{T_I} \int_0^t e(k)dt = K_I \int_0^t e(k)dt$$

The controller used for track following is described by following Eq. 5-1.

Practical model of PID controller

$$U(t) = K_c[(SP - PV) + T_D \frac{d(SP - PV)}{dt} + \frac{1}{T_I} \int_0^t (SP - PV)dt]$$

$$= K_P e(k) + K_D \frac{de(k)}{dt} + K_I \int_0^t e(k)dt \quad (5\text{-}1)$$

The PID controller implemented in LABVIEW codes uses an integral sum correction algorithm that facilitates anti-windup and bumpless manual to automatic transfers. The integral sum correction algorithm prevents abrupt controller output

changes when switching from manual to automatic mode or changing any other parameters. The diagram of PID controller implemented on LABVIEW codes is shown in Figs. 5-2(a) and 5-2(b).

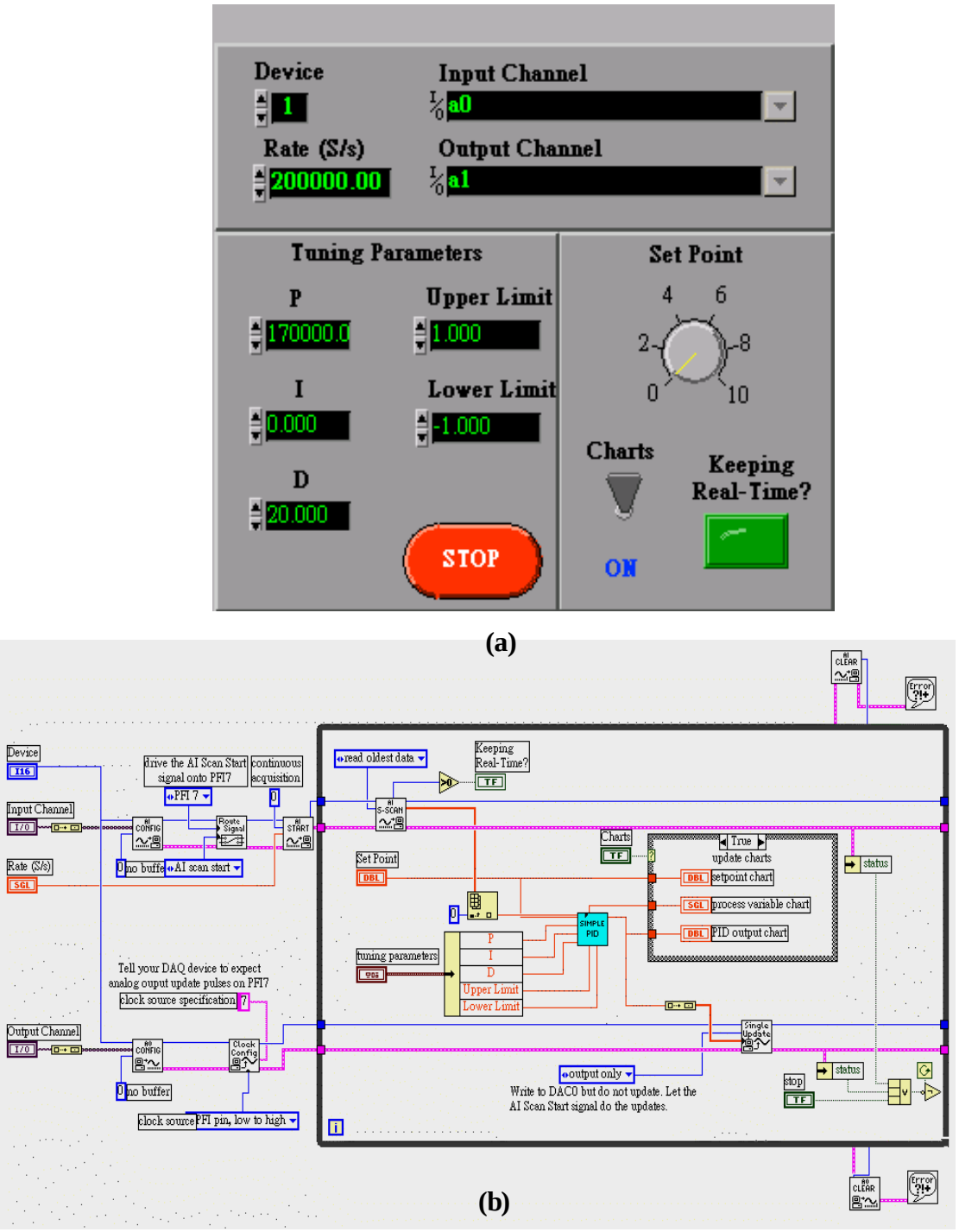

Fig. 5-2 (a) Control panel of PID controller and (b) LABVIEW diagram of PID controller

The PID controller implemented in LABVIEW software can realize tracking

system with AD/DA card. The setpoint SP calculated by push-pull detector is the desired point which is set 0 to wait for the laser spot on track. The process variable PV of the system will be read as an analog input from photo-detector, and the PID output to the system will be generated as an analog output to control micro-mirror. The input and output are hardware-synchronized. Furthermore, because the 200 kHz sampling rate of NI AD/DA card is over 20 times of the tracking system bandwidth **[28]**, the continuous analysis that has been simulated in chapter 4 can be applied here. It can be assured that the digital controller converted by AD/DA card with enough sampling rate will match the performance of continuous controller optimized in Chapter 4. Therefore, according to optimization of tracking system in Chapter 4, the coefficients of PID controller are shown as below:

$$K_P = 170000,\ K_D = 20,\ K_I = 0$$

These optimal parameters are the defaults of the PID controller for tuning tracking system on track in closed loop.

5.2 Optical tracking experiments with MEMS mirror along

A tracking experiment was conducted to demonstrate the tracking improvement by using a MEMS tracking mirror. Assuming that the MEMS mirror will be used in DVD drives, the optical test system consisted of a light source with 660 nm wavelength and an objective lens of 0.6 NA as simulated in Chapter 2. The track pitch of the medium was 0.74um. The rotation speed of the medium was from 500 rpm to 1000 rpm. Designed PID controller was implemented in PC based controller with a sample rate of 200 kHz.

5.2.1 Crossing tracks

The tracking error signals were illustrated in Figs. 5-3 and 5-4 when the tracking servo was switched off and a triangular wave was applied to the MEMS mirror. When the tracking servo is off, the tracking error signal varies because the laser spot crosses the tracks. The distance between two tracks (track pitch) is 0.74 um. Therefore, from Fig. 5-4 as the mirror was driven at 45 mV, the laser spot crossed 10 tracks, which was equal to 7.4 um of tracking distance. The tilt angle of micro-mirror can be calculated to be about 0.01 degree following equation 3.11. In the experiment when the mirror was driven at over than 500 mV, the tracking error signals became much more asymmetric due to optical aberration by mirror's tilt. Too much asymmetry would increase the loading of the control system and unacceptably deteriorate the read-out spot. Therefore, the driving range of tracking mirror is limited to 500 mV to maintain minimum optical quality, with which tracking control system can converge to steady state. This asymmetry may result from the large distance between the photo-detector and the disk in the experiment setup shown in Fig. 3-9. Large distance between photo-detector and disk would hasten the inferiority of optical quality including the tracking error signals. Therefore, if the micro-mirror could be packaged and integrated in pick-up, the optical quality and tracking distance would also be improved.

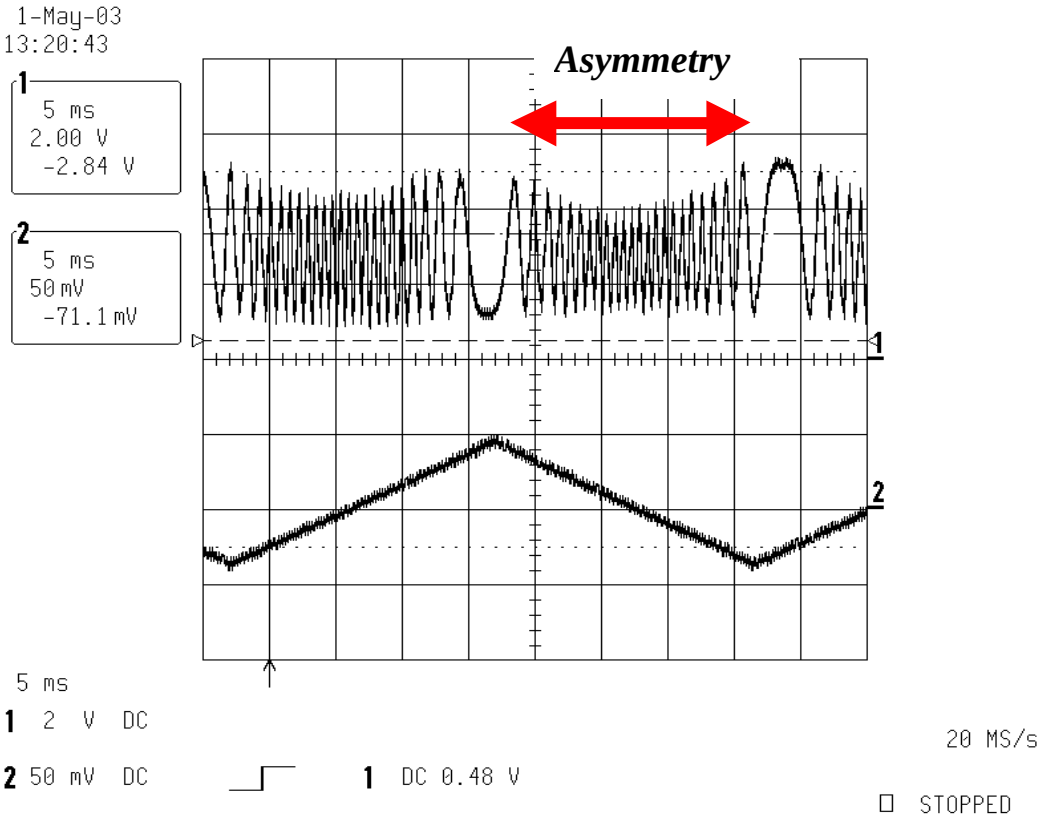

Fig. 5-3 Tracking error signals TES of tracking system

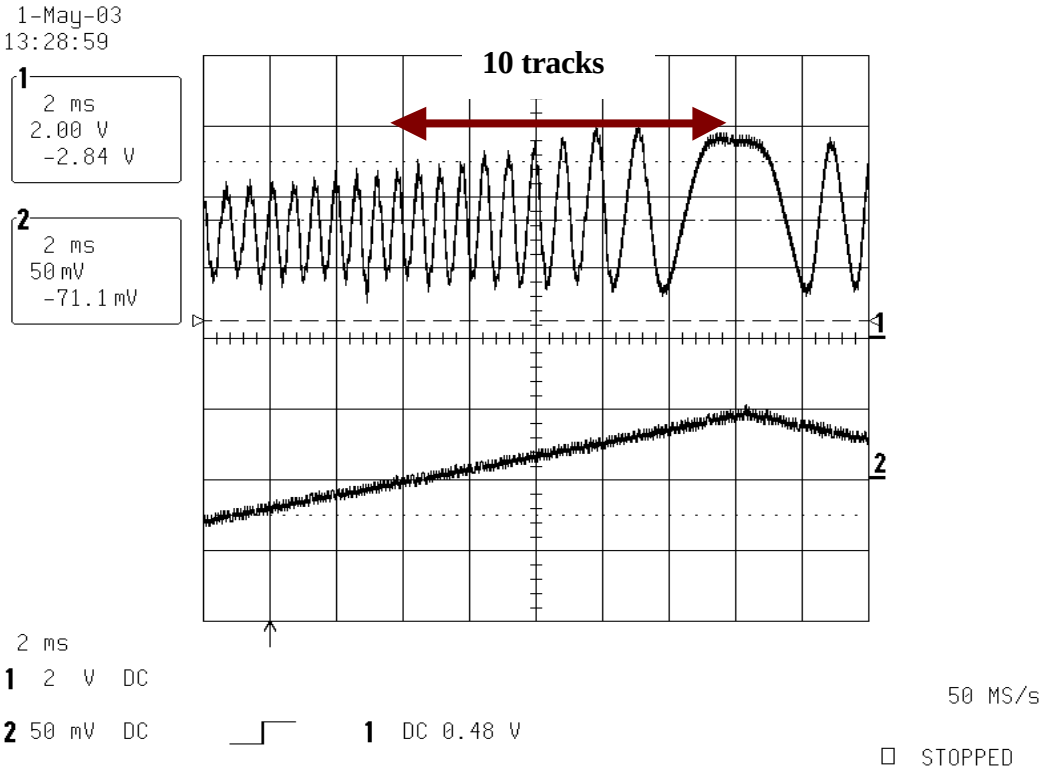

Fig. 5-4 Tracking error signals TES of tracking system (Zoom in)

5.2.2 Closed loop tracking system

In Chapter 4, the optimal coefficients of PID controller were obtained by MATLAB simulation tool. But these coefficients injected to the closed-loop tracking system in practice cannot keep the tracking system within the steady state. It had serious overshoot and oscillation, which would push the system into unstable state as shown in Fig. 5-5. The coefficients of PID controller required retuned.

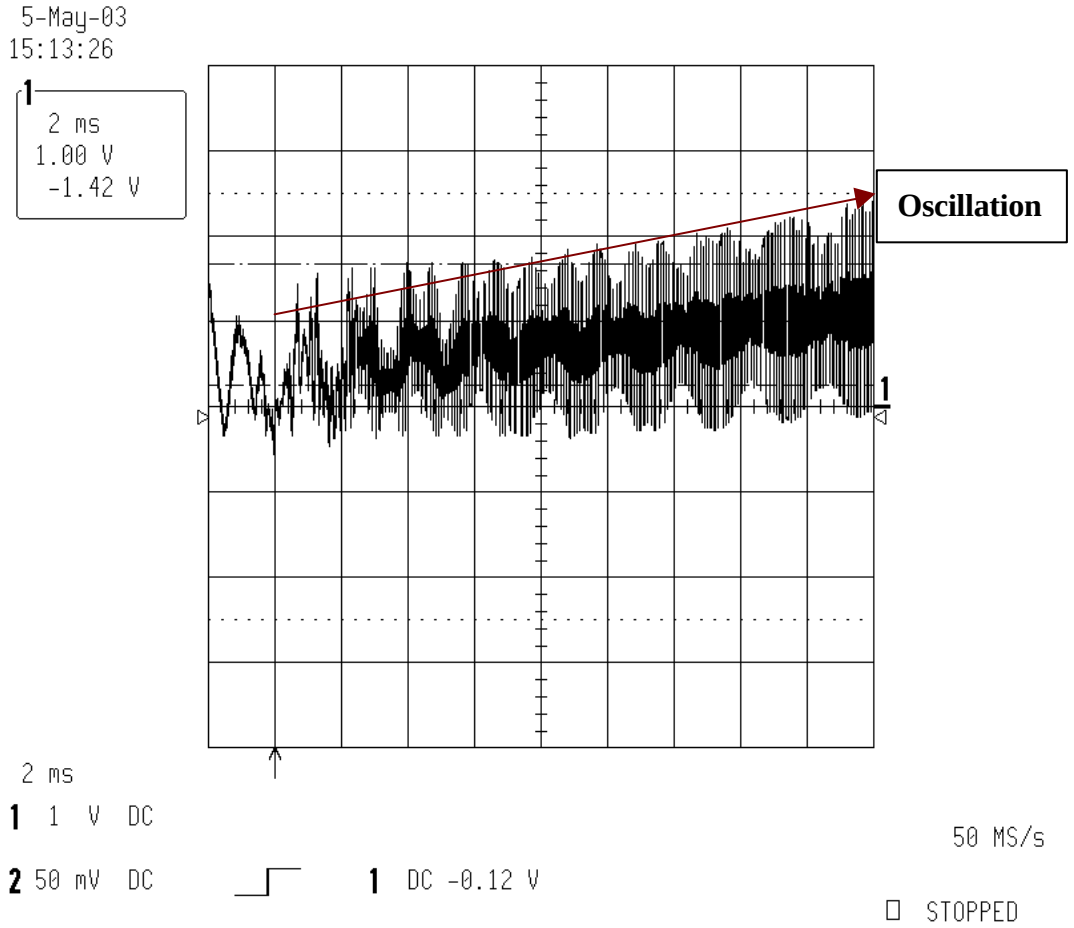

Fig. 5-5 TES of unstable tracking system

According to the criteria for tuning the controller, increasing K_P and K_I tends to reduce system errors but may not be capable of also producing adequate stability, while increasing K_D tends to improve stability. Because the tracking system had error offset and overshoot in steady state shown in Fig. 5-5, we increased K_P and K_D step by step in order to reduce system errors and overshoot. By using this trial-and-error method, the steady-state tracking system was tuned with following coefficients of PID controller. The I controller had not been used in the tracking system.

K_P = 175000, K_D =23, K_I = 0

With such a PD controller, the tracking error signals TES in closed-loop is shown in Fig. 5-7. The Channel 1 is the tracking-mirror control signals and the Channel 2 is the closed-loop tracking error signal (TES) at the rotation speed 100 rpm. From Fig. 5-6, the relation G (V/um) between the distance and voltage of tracking error can be found. According to the experimental result in Fig. 5-4, we can calculate that the distance Z1-Z2 is 0.37 um (half distance between two lands), and the voltage TES_1 -TES_2 is 2.2 V (peak to peak).

$$Slope = G = \frac{TES1 - TES2}{Z1 - Z2} = \frac{2.2V}{0.37um} = 5.95(V/um)$$

According to this relation G, the tracking error of micro-mirror tracking system can be calculated to ± 5nm for ± 30 mV of tracking error signal shown in Fig. 5-7. As a result, the tracking system using the MEMS tracking mirror has improved the tracking errors to ± 5nm.

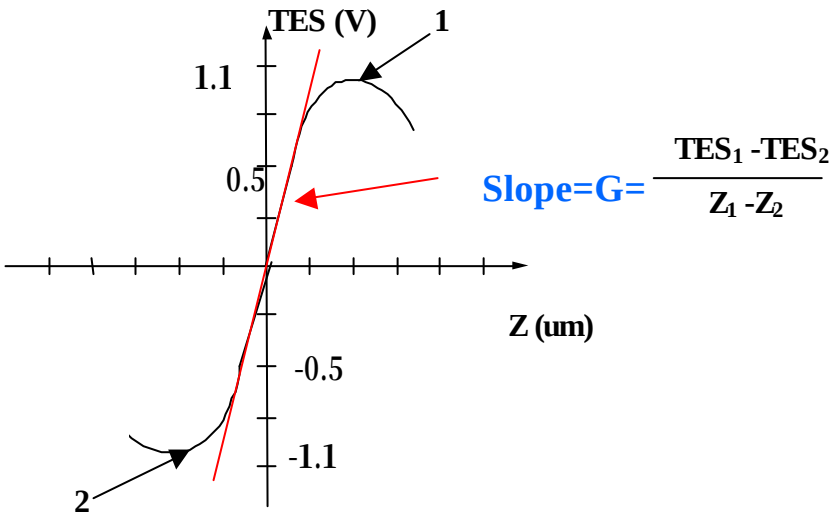

Fig. 5-6 The relation G between the distance and voltage of tracking error

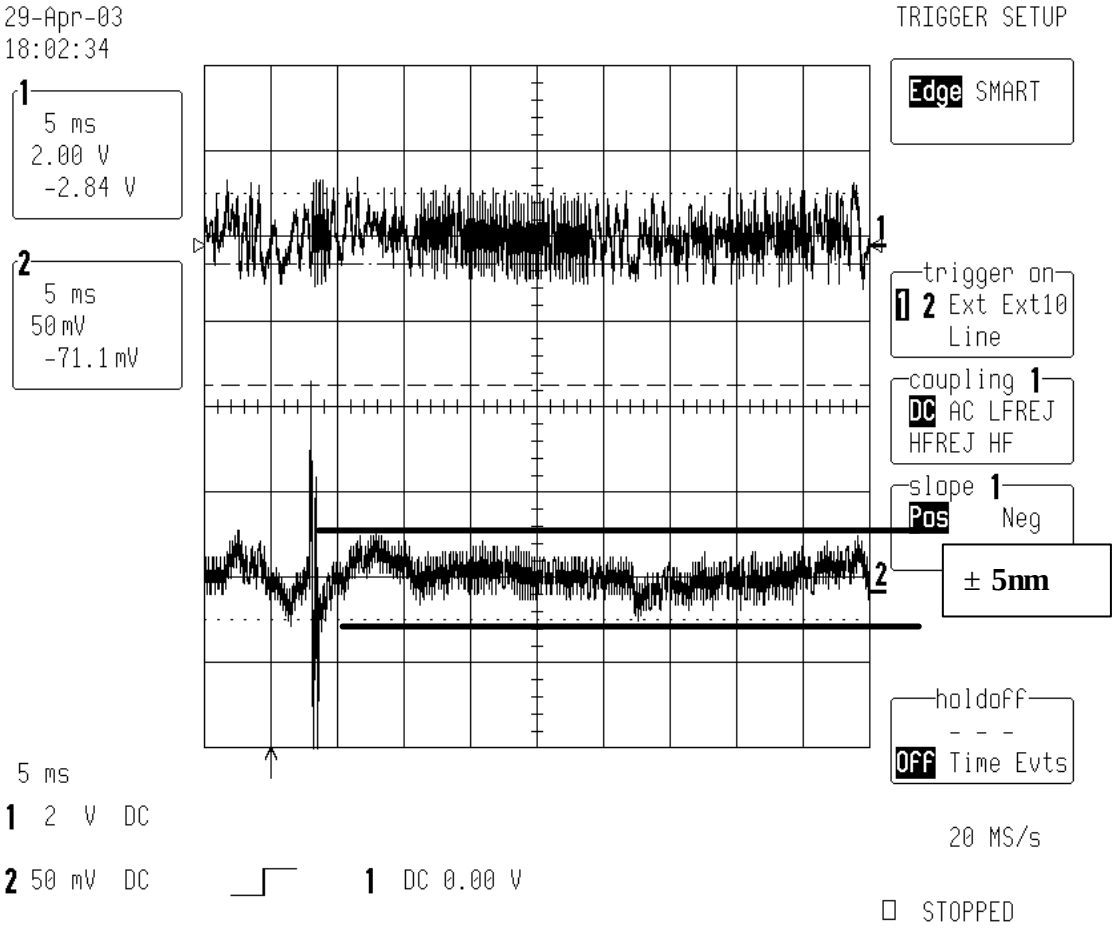

Fig. 5-7 The TES of tracking system in closed-loop at 100 rpm

5.2.3 Tracking comparison between MEMS mirror and voice-coil-motor [29]

The final step in this thesis is to compare the tracking performance between tracking mirror and voice coil motor (VCM). Figs. 5-8 and 5-9 show the tracking errors of mirror and VCM in rotation speed 500 rpm and 1000 rpm. The closed-loop tracking error signals (TES) of MEMS mirror and VCM are set to channel 1 and channel 2. Based on the tracking error signals, the tracking actuator allows the system to respond quickly to pull the spot back to the center of the track. The results in Figs. 5-8 and 5-9 obviously demonstrate that the tracking mirror had the tracking errors of 17 nm and 30 nm in rotation speed 500 rpm and 1000 rpm, while VCM had tracking errors of 80 nm and 120 nm.

5.3 Summary

With the advantages of high bandwidth and loop gain, the mirror can track more precisely and quickly than the VCM. Therefore, we replace the MEMS mirror for VCM to enhance the bandwidth of tracking system. As a result, the comparing results of tracking errors between tracking mirror and VCM demonstrate this assumption and design. The improved tracking performance can truly increase the tracking precision and tolerance, which is required for the future drives with the requirements of high density and data rate.

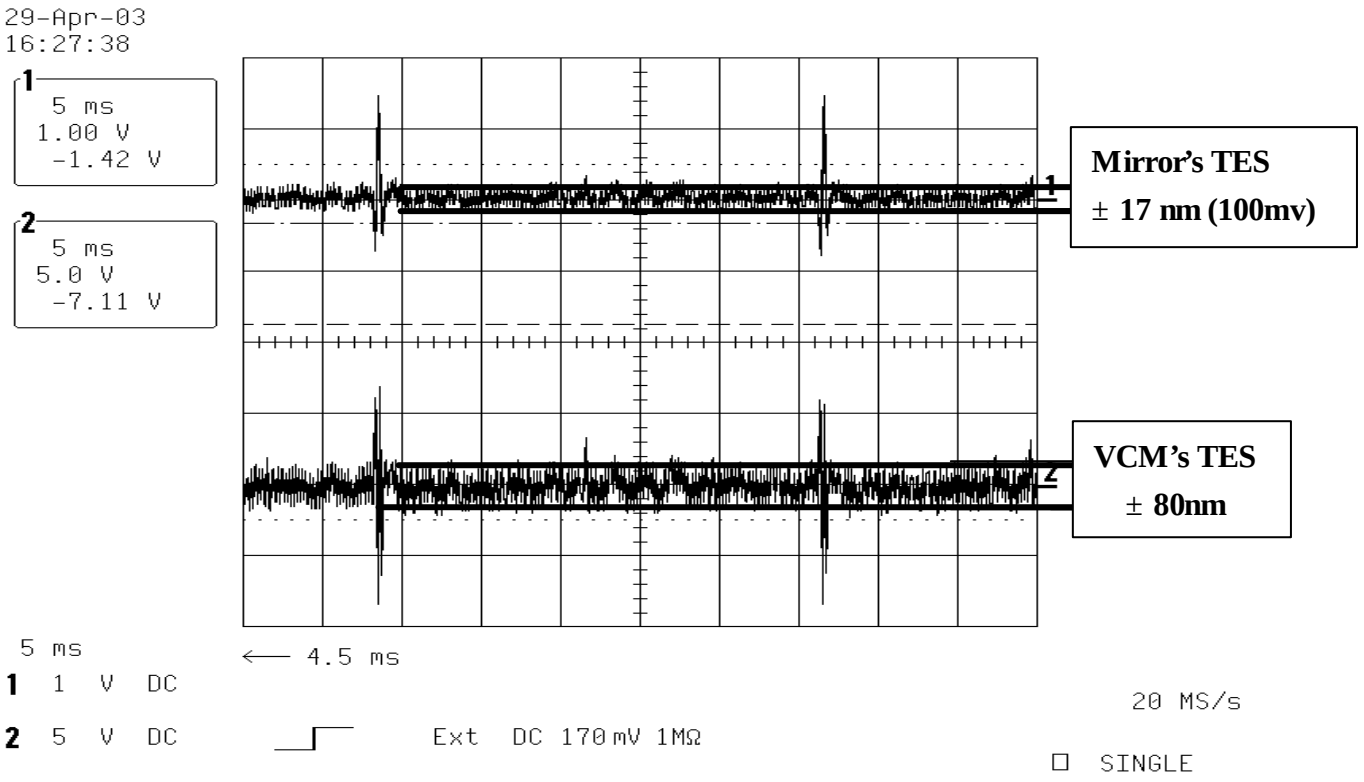

Fig. 5-8 TES of mirror and VCM in 500rpm

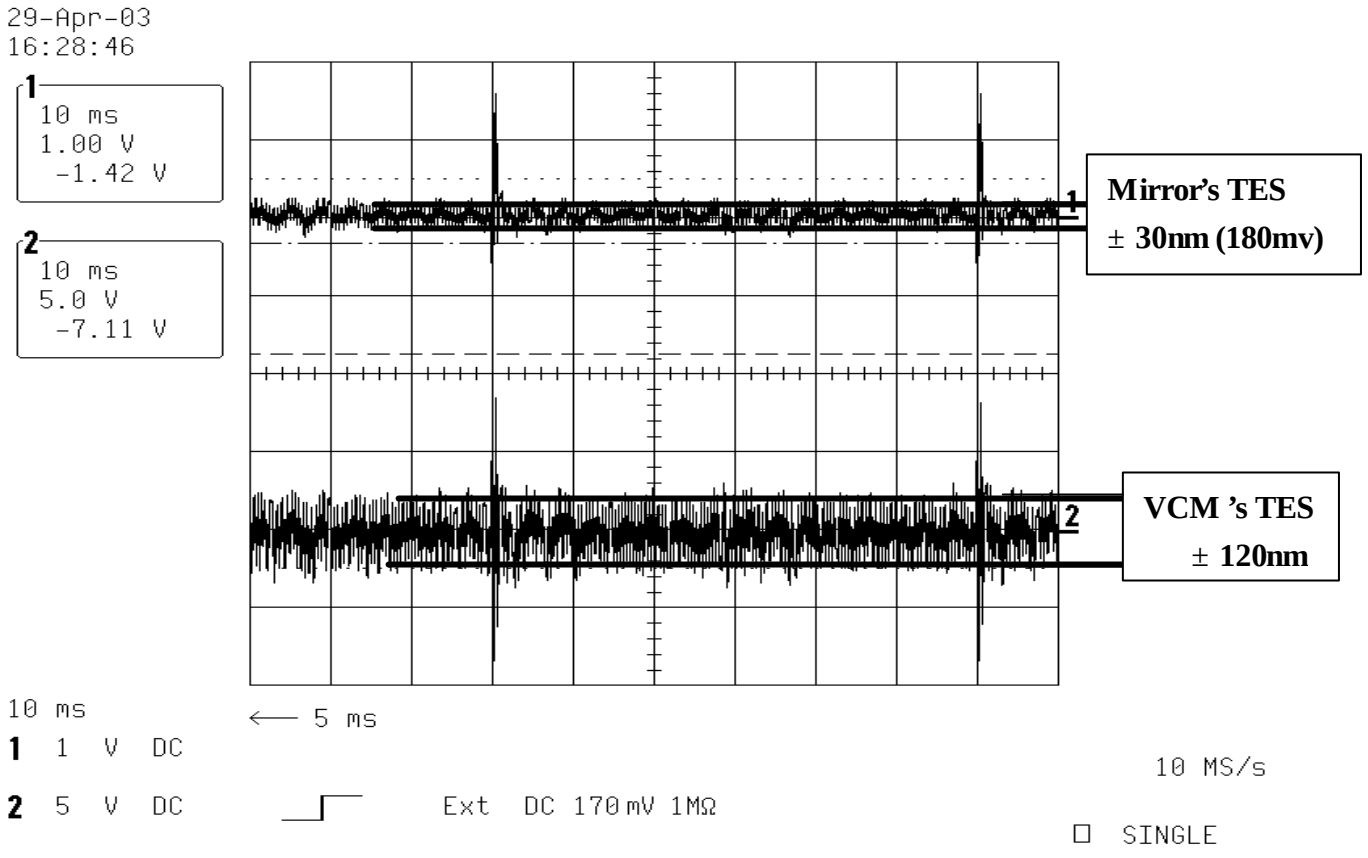

Fig. 5-9 TES of mirror and VCM in 1000rpm